The Astrophysical Journal, 937:89 (5pp), 2022 October 1 https://doi.org/10.3847/1538-4357/ac82ae

Search for Coincident Gravitational-wave and Fast Radio Burst Events from 4-OGC and the First CHIME/FRB Catalog

Yi-Fan Wang (王一帆)[1,2] and Alexander H. Nitz[1,2]
[1] Max-Planck-Institut für Gravitationsphysik (Albert-Einstein-Institut), D-30167 Hannover, Germany; yifan.wang@aei.mpg.de
[2] Leibniz Universität Hannover, D-30167 Hannover, Germany
Received 2022 April 20; revised 2022 July 15; accepted 2022 July 18; published 2022 September 30

Abstract

Advanced LIGO and Virgo have reported 90 confident gravitational-wave (GW) observations from compact-binary coalescences from their three observation runs. In addition, numerous subthreshold GW candidates have been identified. Binary neutron star (BNS) mergers can produce GWs and short-gamma-ray bursts, as confirmed by GW170817/GRB 170817A. There may be electromagnetic counterparts recorded in archival observations associated with subthreshold GW candidates. The CHIME/FRB Collaboration has reported the first large sample of fast radio bursts (FRBs), millisecond radio transients detected up to cosmological distances; a fraction of these may be associated with BNS mergers. This work searches for coincident GWs and FRBs from BNS mergers using candidates from the fourth Open Gravitational-wave Catalog and the first CHIME/FRB catalog. We use a ranking statistic for GW/FRB association that combines the GW detection statistic with the odds of temporal and spatial association. We analyze GW candidates and nonrepeating FRBs from 2019 April 1 to 2019 July 1, when both the Advanced LIGO/Virgo GW detectors and the CHIME radio telescope were observing. The most significant coincident candidate has a false alarm rate of 0.29 per observation time, which is consistent with a null observation. The null results imply, at most, $\mathcal{O}(0.01)\%$–$\mathcal{O}(1)\%$ of FRBs are produced promptly from the BNS mergers.

Unified Astronomy Thesaurus concepts: Gravitational wave astronomy (675); Radio bursts (1339); High energy astrophysics (739)

1. Introduction

Gravitational-wave (GW) observations have opened up a new opportunity for multimessenger astronomy. on 2017 August 17, the Advanced LIGO (The LIGO Scientific Collaboration et al. 2015) and Virgo (Acernese et al. 2015) observatories detected a GW consistent with a binary neutron star (BNS) merger (GW170817; Abbott et al. 2017a, 2017b, 2017c). An associated gamma-ray burst was independently detected by the Fermi Gamma-Ray Burst Monitor (Meegan et al. 2009). Subsequent observations found a broad spectrum of electromagnetic emissions, from X-ray and gamma-ray to optical and radio (Abbott et al. 2017c). The detection has confirmed short-gamma-ray bursts originate from BNS mergers (Goodman 1986; Paczynski 1986; Eichler et al. 1989; Narayan et al. 1992), and has several implications such as measurements of neutron star properties (Abbott et al. 2018; Capano et al. 2020; Dietrich et al. 2020; Landry et al. 2020) and inference of the Hubble constant (Abbott et al. 2017d; Guidorzi et al. 2017; Fishbach et al. 2019; Hotokezaka et al. 2019).

A potential electromagnetic counterpart to GWs is a fast radio burst (FRB), a millisecond-duration radio transient found up to cosmological distances. The first FRB event was identified in 2007 (Lorimer et al. 2007). Later, FRB 121102 (Spitler et al. 2016) showed evidence of repeating FRBs, suggesting a classification of repeaters and apparent nonrepeaters. The possible generation mechanisms for FRBs remain a topic of discussion (for a review, see, e.g., Zhang 2020). The detection of a galactic repeating FRB 200428 from a magnetar (Andersen et al. 2020; Bochenek et al. 2020) associated with hard X-rays and soft gamma-rays (Li et al. 2020; Mereghetti et al. 2020; Ridnaia et al. 2021; Tavani et al. 2021) confirms at least a portion of FRBs originate from magnetars. Nevertheless, some FRBs appear not to repeat, and the origin of nonrepeaters remains under active investigation. In addition to the magnetar flare activities (Popov & Postnov 2007; Metzger et al. 2017, 2019; Margalit et al. 2020), possible mechanisms to produce FRBs include the prompt emission from BNS mergers (Totani 2013; Wang et al. 2016; Sridhar et al. 2021), collisions of neutron stars with asteroids or comets (Geng & Huang 2015), giant pulses from pulsars (Keane et al. 2012), or more exotic scenarios such as cosmic strings (Vachaspati 2008). Of particular interest to this work is the prompt emission of FRBs during the BNS merger because of the possible GW counterpart.

Since entering the advanced detector era, LIGO and Virgo have completed three observation runs. The LIGO-Virgo-KAGRA (LVK) collaboration has reported 90 GW observations from compact-binary coalescences up to the third Gravitational-Wave Transient Catalog (Abbott et al. 2021a). Independent groups have searched the public data (Vallisneri et al. 2015; Abbott et al. 2019b) and reported additional detections (Nitz et al. 2021; Olsen et al. 2022). Nitz et al. (2021) has reported the fourth Open Gravitational-wave Catalog (4-OGC) based on the `PyCBC` pipeline (Nitz et al. 2018). In this work, we analyze the public set of subthreshold candidates from the 4-OGC catalog (Nitz et al. 2021).

The Canadian Hydrogen Intensity Mapping Experiment (CHIME; Amiri et al. 2018) has released the first CHIME/FRB catalog (Amiri et al. 2021), reporting 536 events within 1 yr of observation. For 3 months, from April 1 to July 1 in 2019, the GW detectors Advanced LIGO/Virgo and CHIME were both observing, establishing the opportunity to search for coincident

signals. The data obtained from a single uniform survey also enables straightforward background noise estimation for the GW/FRB association. To examine the hypothesized BNS merger scenario for FRBs, we identify GW triggers within a $+/-100$ s around each FRB in the CHIME catalog. We compute a statistic for each pair of temporally coincident events based on the GW detection statistic and the Bayes' factor measuring the sky localization association. To estimate the false alarm rate of our search, we empirically measure the background noise by artificially sliding the time of CHIME events with respect to LIGO/Virgo by a temporal stride of $\sim$1 day, such that we assume any spatial and temporal association is due to false coincidences.

We analyze the available candidates from the 4-OGC and CHIME/FRB catalog that pass our selection criteria; the most significant associated GW/FRB candidate has a false alarm rate of 0.29 per observation time, $\sim$2.4 months (the duty cycle that at least two GW detectors were observing is 81% from April 1 to July 1 in 2019 and we do not consider single detector GW triggers (Nitz et al. 2020)). We adopt criteria from the GW community that a false alarm rate smaller than 1 per 100 yr is considered as a significant detection, which is used by, e.g., Abbott et al. (2016a), and thus conclude a null result in our GW/FRB search. Our result is consistent with the recent null detection from the LIGO Scientific Collaboration et al. (2022). We estimate the fraction of FRBs that are associated with BNS mergers is at most $\mathcal{O}(0.01)\%$–$\mathcal{O}(1)\%$.

2. Methods for Coincident GW/FRB Search

This section briefly reviews the Bayesian inference of GW events, the selection criteria for GW/FRB candidates, and the statistic to rank the GW/FRB association.

2.1. Bayesian Inference for Gravitational Waves

Given GW time series data $d(t)$, which is a sum of the detector noise $n(t)$ and a GW signal $h(t, \vec{\theta})$ with characterizing parameters $\vec{\theta}$, Bayes' theorem states that

$$P(\vec{\theta}|d, H) = \frac{P(d|\vec{\theta}, H)P(\vec{\theta}|H)}{P(d|H)}, \quad (1)$$

where $P(\vec{\theta}|d, H)$ is the posterior probability distribution for parameters $\vec{\theta}$, $P(\vec{\theta}|H)$ is the prior distribution for $\vec{\theta}$, $P(d|\vec{\theta}, H)$ is the likelihood to obtain the data given a set of model parameters, and $P(d|H)$ is a normalization factor called the evidence, which is an integral of the prior-weighted likelihood marginalized over all the model parameters $\vec{\theta}$

$$P(d|H) = \int P(d|\vec{\theta}, H)P(\vec{\theta}|H)\mathrm{d}\vec{\theta}. \quad (2)$$

H is the underlying hypothesis characterizing the signal detection. The Bayes odds ratio, or the ratio of the evidence of two hypotheses, is

$$\mathcal{B}^1_2 = \frac{P(d|H_1)}{P(d|H_2)}, \quad (3)$$

which quantitatively measures the degree to which hypothesis the data favors.

For Gaussian and stationary noise in GW detectors, the likelihood function is

$$P(d|\vec{\theta}, H) \propto \exp\left[-\frac{1}{2}\sum_i \langle d_i - h_i(\vec{\theta})|d_i - h_i(\vec{\theta})\rangle\right], \quad (4)$$

where $h_i(\vec{\theta})$ is the waveform template of GW given by model H and parameters $\vec{\theta}$, and i represents the ith GW detector. The inner product $\langle a|b\rangle$ is defined to be

$$\langle a|b\rangle = 4\Re\int \frac{a(f)b^*(f)}{S_h(f)}df, \quad (5)$$

where $S_h(f)$ is the one-side noise power spectral density of the GW detector as a function of frequency f.

2.2. Candidate Selection

To search for possible GW/FRB associations, we first select the FRBs from the CHIME/FRB catalog occurring from 2019 April 1 to 2019 July 1; this time range overlaps with the first half of the Advanced LIGO/Virgo third observation run. Since the prompt emissions of FRBs associated with a BNS merger are not expected to repeat (Totani 2013; Wang et al. 2016; Sridhar et al. 2021), we only select the apparent nonrepeaters. One hundred fifty-one FRB events remain from the selection.

The targeted search for GWs from compact-binary coalescence relies on accurately modeling the expected signals to enable their use as templates (Harry et al. 2009). The strain data from GW detectors are match filtered against a bank of templates, and then a detection statistic is assigned for each candidate (Allen et al. 2012). We use subthreshold GW candidates recorded in the public release of the 4-OGC catalog (Nitz et al. 2021). The binary component mass and spin parameters from the best-ranked template are given for each candidate.

We select the GW candidates, again occurring from 2019 April 1 to 2019 July 1, whose component mass ranges from one to two solar masses. We consider GW candidates passing these criteria to potentially arise from BNS mergers. The search template bank for BNSs in 4-OGC targets the magnitude of dimensionless spin in $[-0.05, 0.05]$ aligned with orbital angular momentum (Nitz et al. 2021), because BNSs are not expected to have large spins during merger as suggested by the known GW sources (Abbott et al. 2019a, 2020) and galactic BNSs (Zhu et al. 2018). The search would be sensitive to higher spin sources though because of degeneracy between the effective spin and mass ratio for the GW waveform. Extending the search template bank to cover spin up to 0.5 would require an order of magnitude more templates, and trigger the same scale of more background noise. The search approximately loses $\sim$10% sensitive volume for every order of magnitude in background noise (Brown et al. 2012). Overall, around 3×10^5 subthreshold GW candidates satisfy the selection criteria.

2.3. Ranking Statistic for GW/FRB Association

We rank each GW/FRB pair by combining the GW candidate's ranking statistic with the odds that both observations occur at nearly the same time and from a common sky location, following the same spirit of Nitz et al. (2019) and Ashton et al. (2018). This can be expressed as the sum of the GW detection statistic $\lambda_{\rm gw}$ (Nitz et al. 2017; Davies et al. 2020)

and $\ln \mathcal{B}^{\rm fixsky}_{\rm relaxsky}$:

$$\lambda_{\rm gw+frb} = \lambda_{\rm gw} + \ln \mathcal{B}^{\rm fixsky}_{\rm relaxsky}. \quad (6)$$

The expression of $\lambda_{\rm gw}$ for `PyCBC` is in, e.g., Equation (16) of Davies et al. (2020), which represents the natural logarithm of the ratio between signal rate density and noise rate density for a GW trigger. The ranking statistic itself has a clear physical meaning that combines a detection statistic for GW triggers and an improvement of Bayesian evidence if the GW trigger is indeed from the direction informed by an FRB. We assume that each FRB observation does not arise from noise and so do not include any additional factors for its likelihood.

To obtain $\ln \mathcal{B}^{\rm fixsky}_{\rm relaxsky}$, we first look for temporally coincident pairs by selecting GW triggers occurring within a $+/-$ 100 s window with respect to the epoch of an FRB event using "mjd_inf" given by the CHIME/FRB catalog (Amiri et al. 2021). This time window accounts for the time delay of an FRB due to ionized gas in interstellar and intergalactic media, which is $\mathcal{O}(10)s$ (James et al. 2019). The sky localization of FRBs is much more precise than for each GW candidate; the uncertainty for R.A. and decl. in the CHIME/FRB catalog is at the subdegree level. In contrast, the sky localization uncertainty for GWs is tens to hundreds of square degrees. In this work, we use only the two-dimensional sky position information and do not explicitly account for the GW/FRB distance consistency. We define two competing hypotheses using the GW data.

1. $\mathcal{H}_1$: the sky location of the GW observation is fixed to the R.A. and decl. informed by the temporally associated FRB event;
2. $\mathcal{H}_2$: the sky location of the GW observation is considered unknown with a prior expectation that sources are isotropically distributed.

The Bayesian evidence for the two hypotheses are $P(d|\mathcal{H}_1)$ and $P(d|\mathcal{H}_2)$, respectively, and the natural logarithm of the ratio of $P(d|\mathcal{H}_1)$ and $P(d|\mathcal{H}_2)$ is defined to be $\ln \mathcal{B}^{\rm fixsky}_{\rm relaxsky}$, which quantifies the preference for a GW trigger to originate from the same sky position of the associated FRB.

We use `TaylorF2` (Sathyaprakash & Dhurandhar 1991; Droz et al. 1999; Blanchet 2002; Faye et al. 2012) to model the GW signal $h(\vec{\theta})$ and use the dynamic nested sampler `Dynesty` (Speagle 2020) in `PyCBC Inference` (Biwer et al. 2019) to numerically compute the Bayesian evidence. To simplify the calculation, we fix the component masses and spins of the GW signal model to the values given by the best-ranked templates reported by 4-OGC. We do not expect the sky location will be significantly biased by fixing the mass and spin given the decoupling of intrinsic and extrinsic parameters (Singer & Price 2016). Therefore, the variables to infer are the luminosity distance, inclination angle between the total angular momentum direction of the BNS and the line of sight toward the detectors, polarization angle, coalescence time, and phase, for the model $\mathcal{H}_1$. The hypothesis $\mathcal{H}_2$ adds two more variables, the R.A., and decl.. The prior for luminosity distance is from a uniform distribution of comoving volume and is up to 450 Mpc. The priors for angular variables are isotropically distributed.

To determine the false alarm rate of our search as a function of our ranking statistic, we need the background of chance GW/FRB associations. The estimation is achieved by artificially shifting the time of FRB events with respect to the GW triggers by a time much larger than 100 s (we choose ∼1 day as a stride). Since we have assumed that GW/FRB can only be associated within the $+/-100$ s window, any coincident association after time sliding is due to a false coincidence. Using this method, we simulate ∼20 yr of background.

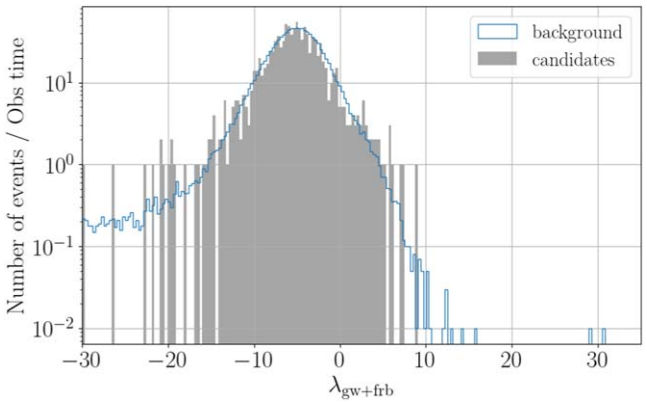

Figure 1. Histogram of the detection statistic values for our search candidates and background noise. The *y*-axis represents the number of events per observation time of 2.4 months, and the bin width is 0.3. The most significant trigger has a $\lambda_{\rm gw+frb} = 8.92$ with a false alarm rate 0.29 per observation time.

Table 1
The Gravitational-wave Trigger Name, the Fast Radio Burst Events, the Detection Statistic and False Alarm Rate (FAR) per Observation Time, Which Is 2.4 Months, for the Top Three Significant Candidates

GW Triggers	FRB Events	$\ln \mathcal{B}^{\rm fixsky}_{\rm relaxsky}$	$\lambda_{\rm gw+frb}$	FAR per Obs
190701_223118	FRB 20190701E	3.97	8.92	0.29
190605_021909	FRB 20190605C	3.64	7.50	0.63
190411_050213	FRB 20190411B	3.27	6.95	0.93

3. Search Results and Implications

We compute $\lambda_{\rm gw+frb}$ for all associated pairs of GW/FRBs. The search candidates and estimated background noise are shown in Figure 1. The GW event name, the FRB events name, the detection statistic, and the false alarm rate for the top three significant candidates are given in Table 1. A complete list of candidates is provided in the associated data release (Wang & Nitz 2022).

The most significant candidate is from the GW trigger 190701_223118 (the name is in the format of YYMMDD_HHMMSS for UTC time) associated with FRB 20190701E, which occurred 22 s later than the GW candidate. The coincident candidate has $\ln \mathcal{B}^{\rm fixsky}_{\rm relaxsky} \sim 3.97$. Figure 2 shows the posterior of sky location for 190701_223118 inferred from the LIGO/Virgo data along with the sky location reported for FRB 20190701E (CHIME/FRB Collaboration 2018). However, the associated false alarm rate is 0.29 per the (2.4 months) observation time. In addition, if we further assume the interstellar and intergalactic medium model given by James et al. (2019), the dispersion measure of FRB 20190701E (CHIME/FRB Collaboration 2018) corresponds to a luminosity distance of ∼3.6 Gpc; in contrast the GW posterior for luminosity distance gives 300^{+100}_{-120} Mpc for 190701_223118. We find no confident associations between GW and FRB candidates from the 4-OGC and CHIME/FRB catalogs.

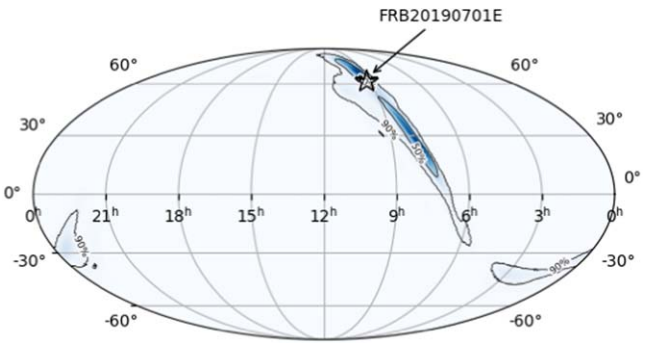

Figure 2. The posterior distribution of sky location for 190701_223118 from Bayesian inference given hypothesis $\mathcal{H}_2$, which assumes the R.A. and decl. are free parameters to be inferred by gravitational-wave strain data. The 90% and 50% credible regions are shown. The marker represents the sky location of FRB 20190701E measured by the CHIME/FRB Collaboration (2018).

Given the null search results, we constrain the rate of coincident GW/FRB observations. Callister et al. (2016) has estimated the physical FRB rate per comoving volume as (their Equation (1))

$$R_{\rm FRB} = 3r_{\rm obs}/(\eta\Omega D^3), \tag{7}$$

where $r_{\rm obs}$ is the observed FRB rate, D is the comoving distance encompassing the observed FRB, η is the detection efficiency in the range [0, 1] and Ω is the opening solid angle of FRB beam from BNS mergers. Based on the observed FRB events and the beam area of the FAST radio telescope, Niu et al. (2021) estimated the all-sky FRB rate to be $r_{\rm obs} = 10^5$ day^{-1} sky^{-1}. We take $D = 5.4$ Gpc from the most distant FRB detected by Niu et al. (2021). Thus the lowest event rate density for FRBs is 5.6×10^4 Gpc^{-3} yr^{-1} assuming the most optimal 100% detection efficiency and $\Omega = 4\pi$. Taking a more realistic assumption given by Callister et al. (2016) that takes account for a lower detection efficiency $\eta = 50\%$ and an opening angle 30° ($\Omega \simeq 0.8$), the FRB event rate density increases to 1.7×10^6 Gpc^{-3} yr^{-1}.

The BNS merger rate from the 4-OGC catalog is estimated to be 200^{+309}_{-148} Gpc^{-3} yr^{-1} (90% credible intervals; Nitz et al. 2021) if we consider GW170817 (Abbott et al. 2017a) and GW190425 (Abbott et al. 2020) to be representative members of a standard BNS population. We thus take 509 Gpc^{-3} yr^{-1} to be the upper limit of event rate density of BNS mergers that are associated with FRBs. Taking the lowest FRB event rate density indicates at most $\mathcal{O}(1\%)$ of FRBs can originate from prompt emission of BNS mergers. A more realistic estimation for FRB event rate suggests BNS mergers can only take account for $\mathcal{O}(0.01\%)$ of FRBs.

4. Discussion and Conclusion

We have searched for temporally and spatially coincident GW and FRB candidates from the public 4-OGC and CHIME/FRB catalogs. Based on a ranking statistic accounting for the GW trigger significance and the odds of sky position association, the most significant coincident pair has a false alarm rate of 0.29 per observation time. Thus no confident detections are made. We estimate up to $\mathcal{O}(0.01)\%$–$\mathcal{O}(1)\%$ of FRBs can be accounted for by BNS mergers through an order of magnitude comparison of the observed BNS merger rate from GW observations and estimates of the FRB event rate. The most optimal fraction $\mathcal{O}(1)\%$ implies $\sim\mathcal{O}(1)$ FRBs in our search are expected to be accompanied by a GW signal; however, it may be beyond the horizon distance of the current GW observatories.

Improved understanding and modeling of the joint properties of a potential GW/FRB observation may be able to further increase the sensitivity of future analyses. For example, the time delay between the associated GW and FRB was chosen to be uniform in a $+/-100$ s window. Future work may enable a more realistic time delay distribution that can be accounted for directly in the ranking statistic. We did not consider the detection probability of each FRB in the statistic, effectively setting all events on the same footing and assuming that none arise from noise. In addition, if only a small portion of FRBs arise from prompt BNS mergers, there may be features in the observed emission that enable distinguishing FRB mechanisms; we currently limit to only excluding repeating sources. Future work may also be able to take into account the FRB dispersion measure into a combined statistic.

Our detection statistic can also be straightforwardly applied to search for coincident binary black hole mergers and FRBs, given models that predict charged black hole mergers may produce FRBs (Zhang 2016; Liu et al. 2016). Future work can also search GWs associated with repeating FRBs powered by a neutron star formed after the BNS merger, as predicted by Wang et al. (2020) and Zhang et al. (2020). Multimessenger searches could also include neutrinos from the IceCube catalogs (IceCube Collaboration et al. 2021) or gamma-ray burst counterparts (Nitz et al. 2019; Abbott et al. 2021b, 2022).

The fourth observation run of Advanced LIGO/Virgo/KAGRA is scheduled to start on 2023 March (Abbott et al. 2016b); the BNS horizon distance is expected to expand to 160–190 Mpc for LIGO, compared with the horizon distance of 120–140 Mpc in the third observation run (Abbott et al. 2021a). The improved detectors have the potential to observe GW170817-like multimessenger observations and provide tighter constraints on the BNS merger/FRB association event rate or even make the first detection for GW and FRB multimessenger astronomy.

A complete list of search candidates and scripts associated with this work is released in Wang & Nitz (2022).

We acknowledge the Max Planck Gesellschaft and the Atlas cluster computing team at AEI Hannover for support. This research has made use of data, software, and/or web tools obtained from the Gravitational Wave Open Science Center (https://www.gw-openscience.org), a service of LIGO Laboratory, the LIGO Scientific Collaboration, and the Virgo Collaboration. LIGO is funded by the U.S. National Science Foundation. Virgo is funded by the French Centre National de Recherche Scientifique (CNRS), the Italian Istituto Nazionale della Fisica Nucleare (INFN), and the Dutch Nikhef, with contributions by Polish and Hungarian institutes.

ORCID iDs

Yi-Fan Wang (王一帆) https://orcid.org/0000-0002-2928-2916
Alexander H. Nitz https://orcid.org/0000-0002-1850-4587

References

Abbott, B. P., Abbott, R., Abbott, T. D., et al. 2016a, PhRvX, 6, 041015
Abbott, B. P., Abbott, R., Abbott, T. D., et al. 2016b, LRR, 19, 1

Abbott, B. P., Abbott, R., Abbott, T. D., et al. 2017a, PhRvL, 119, 161101
Abbott, B. P., Abbott, R., Abbott, T. D., et al. 2017b, ApJL, 848, L13
Abbott, B. P., Abbott, R., Abbott, T. D., et al. 2017c, ApJL, 848, L12
Abbott, B. P., Abbott, R., Abbott, T. D., et al. 2017d, Natur, 551, 85
Abbott, B. P., Abbott, R., Abbott, T. D., et al. 2018, PhRvL, 121, 161101
Abbott, B. P., Abbott, R., Abbott, T. D., et al. 2019a, PhRvX, 9, 011001
Abbott, B. P., Abbott, R., Abbott, T. D., et al. 2020, ApJL, 892, L3
Abbott, R., Abbott, T. D., Abraham, S., et al. 2019b, SoftX, 13, 100658
Abbott, R., Abbott, T. D., Abraham, S., et al. 2021b, ApJ, 915, 86
Abbott, R., Abbott, T. D., Acernese, F., et al. 2021a, arXiv:2111.03606
Abbott, R., Abbott, T. D., Acernese, F., et al. 2022, ApJ, 928, 2
Acernese, F., Agathos, M., Agatsuma, K., et al. 2015, CQGra, 32, 024001
Allen, B., Anderson, W. G., Brady, P. R., Brown, D. A., & Creighton, J. D. E. 2012, PhRvD, 85, 122006
Ashton, G., Burns, E., Dal Canton, T., et al. 2018, ApJ, 860, 6
Biwer, C. M., Capano, C. D., De, S., et al. 2019, PASP, 131, 024503
Blanchet, L. 2002, LRR, 5, 3
Bochenek, C. D., Ravi, V., Belov, K. V., et al. 2020, Natur, 587, 59
Brown, D. A., Harry, I., Lundgren, A., & Nitz, A. H. 2012, PhRvD, 86, 084017
Callister, T., Kanner, J., & Weinstein, A. 2016, ApJL, 825, L12
Capano, C. D., Tews, I., Brown, S. M., et al. 2020, NatAs, 4, 625
Davies, G. S., Dent, T., Tápai, M., et al. 2020, PhRvD, 102, 022004
Dietrich, T., Coughlin, M. W., Pang, P. T. H., et al. 2020, Sci, 370, 1450
Droz, S., Knapp, D. J., Poisson, E., & Owen, B. J. 1999, PhRvD, 59, 124016
Eichler, D., Livio, M., Piran, T., & Schramm, D. N. 1989, Natur, 340, 126
Faye, G., Marsat, S., Blanchet, L., & Iyer, B. R. 2012, CQGra, 29, 175004
Fishbach, M., Gray, R., Magaña Hernandez, I., et al. 2019, ApJL, 871, L13
Geng, J. J., & Huang, Y. F. 2015, ApJ, 809, 24
Goodman, J. 1986, ApJL, 308, L47
Guidorzi, C., Margutti, R., Brout, D., et al. 2017, ApJL, 851, L36
Harry, I. W., Allen, B., & Sathyaprakash, B. 2009, PhRvD, 80, 104014
Hotokezaka, K., Nakar, E., Gottlieb, O., et al. 2019, NatAs, 3, 940
IceCube Collaboration, Abbasi, R., Ackermann, M., et al. 2021, arXiv:2101.09836
James, C. W., Anderson, G. E., Wen, L., et al. 2019, MNRAS, 489, L75
Keane, E. F., Stappers, B. W., Kramer, M., & Lyne, A. G. 2012, MNRAS, 425, L71
Landry, P., Essick, R., & Chatziioannou, K. 2020, PhRvD, 101, 123007
Li, C. K., Lin, L., Xiong, S. L., et al. 2020, NatAs, 5, 378
Liu, T., Romero, G. E., Liu, M.-L., & Li, A. 2016, ApJ, 826, 82
Lorimer, D. R., Bailes, M., McLaughlin, M. A., Narkevic, D. J., & Crawford, F. 2007, Sci, 318, 777
Margalit, B., Beniamini, P., Sridhar, N., & Metzger, B. D. 2020, ApJL, 899, L27
Meegan, C., Lichti, G., Bhat, P. N., et al. 2009, ApJ, 702, 791
Mereghetti, S., Savchenko, V., Ferrigno, C., et al. 2020, ApJL, 898, L29
Metzger, B. D., Berger, E., & Margalit, B. 2017, ApJ, 841, 14
Metzger, B. D., Margalit, B., & Sironi, L. 2019, MNRAS, 485, 4091
Narayan, R., Paczynski, B., & Piran, T. 1992, ApJL, 395, L83
Nitz, A. H., Dent, T., Dal Canton, T., Fairhurst, S., & Brown, D. A. 2017, ApJ, 849, 118
Nitz, A. H., Dent, T., Davies, G. S., & Harry, I. 2020, ApJ, 897, 169
Nitz, A. H., Harry, I. W., Willis, J. L, et al. 2018, PyCBC Software, GitHub, https://github.com/gwastro/pycbc
Nitz, A. H., Kumar, S., Wang, Y.-F., et al. 2021, arXiv:2112.06878
Nitz, A. H., Nielsen, A. B., & Capano, C. D. 2019, ApJL, 876, L4
Niu, C.-H., Li, D., Luo, R., et al. 2021, ApJL, 909, L8
Olsen, S., Venumadhav, T., Mushkin, J., et al. 2022, PhRvD, 106, 043009
Paczynski, B. 1986, ApJL, 308, L43
Popov, S. B., & Postnov, K. A. 2007, arXiv:0710.2006
Ridnaia, A., Svinkin, D., Frederiks, D., et al. 2021, NatAs, 5, 372
Sathyaprakash, B. S., & Dhurandhar, S. V. 1991, PhRvD, 44, 3819
Singer, L. P., & Price, L. R. 2016, PhRvD, 93, 024013
Speagle, J. S. 2020, MNRAS, 493, 3132
Spitler, L. G., Scholz, P., Hessels, J. W. T., et al. 2016, Natur, 531, 202
Sridhar, N., Zrake, J., Metzger, B. D., Sironi, L., & Giannios, D. 2021, MNRAS, 501, 3184
Tavani, M., Casentini, C., Ursi, A., et al. 2021, NatAs, 5, 401
The CHIME/FRB Collaboration 2018, FRB 20190701E, https://www.chime-frb.ca/catalog/FRB20190701E
The CHIME/FRB Collaboration,, Amiri, M., Bandura, K., et al. 2018, ApJ, 863, 48
The CHIME/FRB Collaboration, Amiri, Mandana, Andersen, Bridget C., et al. 2021, ApJS, 257, 59
The CHIME/FRB Collaboration., Andersen, B. C., Bandura, K. M, et al. 2020, Natur, 587, 54
The LIGO Scientific Collaboration, Aasi, J., Abbott, B. P., et al. 2015, CQGra, 32, 074001
The LIGO Scientific Collaboration, the Virgo Collaboration, the KAGRA Collaboration, et al. 2022, arXiv:2203.12038
Totani, T. 2013, PASJ, 65, L12
Vachaspati, T. 2008, PhRvL, 101, 141301
Vallisneri, M., Kanner, J., Williams, R., Weinstein, A., & Stephens, B. 2015, JPhCS, 610, 012021
Wang, F. Y., Wang, Y. Y., Yang, Y.-P., et al. 2020, ApJ, 891, 72
Wang, J.-S., Yang, Y.-P., Wu, X.-F., Dai, Z.-G., & Wang, F.-Y. 2016, ApJL, 822, L7
Wang, Y. F., & Nitz, A. H. 2020, Data release associated with this work, https://github.com/gwastro/gwfrb-4ogc-chime
Zhang, B. 2016, ApJL, 827, L31
Zhang, B. 2020, Natur, 587, 45
Zhang, G. Q., Yi, S. X., & Wang, F. Y. 2020, ApJ, 893, 44
Zhu, X., Thrane, E., Osłowski, S., Levin, Y., & Lasky, P. D. 2018, PhRvD, 98, 043002